

# Image Deblurring Methodology using Wiener Filter & Genetic Algorithm

Prem Krishan Rana<sup>1</sup>, Deepak Jhanwar<sup>2</sup>

<sup>1</sup>M. Tech. Scholar (D.C), Engineering College, Ajmer, India  
Ranapremkrishan@gmail.com

<sup>2</sup>Assistant Professor, Engineering College Ajmer, India

**Abstract**— The Blind Image Deconvolution/ Deblurring (BID) issue was acknowledged in the mid1960 yet despite everything it stays a difficult errand for the picture handling research network to locate an effective, solid and in particular a differently relevant deblurring plan.

This exploration is centered on the improvement of rebuilding plans for genuine obscured pictures. The essential target is to structure a BID plan that is powerful in term of Point Spread Function (PSF) estimation, proficient as far as rebuilding speed, and viable as far as reclamation quality. An ideal plan will require a deblurring measure to go about as a criticism of value with respect to the deblurred picture and lead the estimation of the obscuring PSF. The obscured picture and the assessed PSF would then be able to be passed on to any traditional reclamation channel for deblurring.

The deblurring measures exhibited in this exploration incorporate visually impaired non-Gaussianity measures just as visually impaired Image Quality Measures (IQMs). These measures are visually impaired as in they can check the nature of a picture straightforwardly from it iii without the need to reference a brilliant picture. The non-Gaussianity measures incorporate spatial and phantom kurtosis measures; while the picture quality analyzers incorporate the Blind/Reference-less Image Spatial Quality Evaluator (BRISQUE), Natural Image Quality Evaluator (NIQE) record and Re-obscuring based Peak Signal to Noise Ratio (RPSNR) measure. Likewise, parametric and self-assertively molded (non-parametric or conventional) PSFs were treated for the visually impaired deconvolution of pictures. Full-reference and non-reference IQMs have been used to check the nature of deblurred pictures for the BID plans.

The essentialness of the examination work lies in the BID plan's capacity to deal with parametric and self-assertively molded PSFs utilizing a solitary calculation, for single-shot obscured pictures, with improved streamlining through GA related to different input IQMs.

**Keywords**— Image Deblurring, Wiener Filter, Genetic Algorithm.

## I. INTRODUCTION

Image Blurring has become a serious point of concern with the advancement of technologies. Such issues arise from various sources such as handheld cameras, mobile camera, CCTV, satellite sources, sometimes from other sources as well. The process of capturing plays a vital role in quality of any image. If recorded with imperfections, this leads into several issues later on while processing such images to obtain relevant information out of them. These issues are mainly occurring because of lens defocusing, improper lighting. The use of handheld cameras, especially by amateur photographers, has resulted in blurred images caused mostly from camera shake or improper focus of camera lens. Some examples of such blurred images are shown in Fig.



Fig 1: Example of Realistic Blurred Images

Furthermore, noise may corrupt any captured image. Noise may appear due to the inability of the models to estimate the imaging data perfectly and is regarded as deblurring noise. Apart from noise, ringing may occur in the restored image due to the imperfect estimation of blur. Ringing occurs for a restoration filter if it assumes the image's frequency sample is periodic which leads to high frequency drop-off at the image boundaries. Removing or correcting such issues of imperfections, becomes very important when it comes about Image Processing or may be Signal Processing.

## II. LITERATURE SURVEY

The literature survey reveals that a lot of work has been done for Image Deblurring. During processing framework many points are not touched. In this work such points are covered which have not been considered by the researchers in the past with the following objectives:

- To identify the major challenges in Image Deblurring.
- To propose a method for reducing computation time and increasing accuracy.
- To provide more relevant results

1. **Chengtao Cai, An Liu, Baolu Zhang [2016]** proposed a Motion Image Deblurring System with Wiener Filter Algorithm. The key methodology in the framework was to examine the range of the Fourier change to assess the point spread capacity of the obscured picture and reestablish the picture in victor channel. In Wiener channel calculation, distinctive parameter has diverse impact on the picture and the impact of different parameters were recorded and broke down by them. The wiener filter was proposed as simple, efficient and good influencing algorithm for image restoration. The major concern with approach is the degradation of image quality after restoration of image.

2. **Yuquan Xu, Xiyuan Hu, Silong Peng [2015]**, proposed a Blind movement deblurring utilizing optical stream model. This work underscored on two sort of movement obscure, including Camera Shake and moving items. The real commitments were including the reconciliation of the scene that has experienced a relative movement depicted by a grouping of optical stream fields. Likewise, they determined the optical stream estimation calculation to help gauge the non-uniform PSF for every pixel. Various constraints were applied on the images to obtain good results in different conditions. The speed of execution was a major concern in the work.

3. **F.Alaoui, A. Ghlaifan Abdo Saleh, V.Dembele, A.Nassim [2014]**, proposed a paper on Application of Blind Deblurring Algorithm for Face Biometric. The key areas of concern were deblurring of motion blurred images during face biometric using blind deblurring techniques. Sparse Kernel Estimation using Salient Edge Prediction, Estimation of Blur Kernel and ISD based Kernel Refinement was done and finally a Fast TV 11 Deconvolution was performed. Euclidean distance was calculated to obtain the difference between original and motion blurred images as performance evaluation. The major drawback of this work was related to non-linear motion blurred images (the variation of both direction and size of blur).

4. **C. Y. Zhou, S. Lin, and S. K. Nayar, [2011]**, proposed a paper on Coded Aperture Pairs for Depth from Defocus and Defocus Deblurring, expressing that, the traditional way to deal with profundity from defocus (DFD) utilizes focal points with round openings for picture catching. The utilization of a round opening seriously limits the precision of DFD was appeared. The basis for assessing a couple of openings as for the exactness of profundity recuperation was determined in it. This basis is upgraded utilizing a hereditary calculation and angle plunge search to touch base at a couple of High-goals openings. These two coded openings are found to supplement each other in the scene frequencies they safeguard. This property empowers them to recuperate profundity with more noteworthy loyalty as well as get a superb all engaged picture from the two caught pictures. Broad reproductions just as tests on an assortment of genuine scenes exhibit the advantages of utilizing the coded openings over traditional roundabout gaps.

5. **Aftab Khan, Hujun Yin, [2018]**, proposed paper on Parametric visually impaired picture deblurring with inclination based unearthy kurtosis expansion expressing, A steepest plunge streamlining plan is utilized to enhance the haze parameter toward most extreme supreme kurtosis of the deblurred picture. The proposed technique works on single picture and is straightforward, effective and simple to execute. The strategy is relevant to different kinds of foggy spots, for example, Gaussian, movement and out-of-center. Examinations on both counterfeit and genuine obscured pictures have demonstrated the capacity and checked improvement of the plan over the current

techniques, as far as both visual recognition and a scope of value measures.

6. **R. Raskar, A. Agrawal, and J. Tumblin [2006]**, introduced paper on Coded Exposure Photography: Motion Deblurring Using Fluttered Shutter. In an ordinary single-presentation photo, moving items or moving cameras cause movement obscure. The introduction time characterizes a fleeting box channel that spreads the moving item over the picture by convolution. They show that physically determined point spread capacities are adequate for a few testing instances of movement obscure evacuation including incredibly enormous movements, finished foundations and fractional occludes.
7. **O. Whyte [2012]**, in paper titled as, Non-uniform Deblurring for Shaken Images, expressed that, Photographs taken in low-light conditions are regularly hazy because of camera shake, for example a movement of the camera while its shade is open. Most existing deblurring techniques model the watched foggy picture as the convolution of a sharp picture with a uniform haze part. This model can catch non-uniform haze in a picture because of camera shake utilizing a solitary worldwide descriptor, and can be substituted into existing deblurring calculations with just little adjustments. To show its viability, it was connected this model to two deblurring issues; first, the situation where a solitary foggy picture is accessible, for which we look at both an estimated minimization approach and a most extreme a posteriori approach, and second, the situation where a sharp however boisterous picture of the scene is accessible notwithstanding the hazy picture. Makes it conceivable to display and evacuate a more extensive class of hazy spots than past methodologies, including uniform haze as an exceptional case, and exhibit its adequacy with tests on engineered and genuine pictures.

### III. RESEARCH METHODOLOGY

The field of BID spans over a period of four decades and has applications in diverse fields. A wide range of mathematical and image processing techniques were used to tackle this. This section is committed to place a look at some essential ideas in the field of BID. The Degradation Model, Types of Blurs, and a Filters of Restorations are discussed. Some of the existing techniques are also discussed to compare the current research work.

#### Problem Formulation

Accepting picture rebuilding process as a straight framework, a caught picture is the yield of the convolution of the spatial drive reaction otherwise called Point Spread Function (PSF) of the direct obscuring framework with the first picture (scene).

Give  $m$  and  $n$  a chance to be the spatial picture directions and  $f$  present the first picture with no type of corruption,  $h$  be the PSF and the yield of the framework be given by  $g$ . Scientifically, for a stationary impulse response of the system over the picture (for example a spatially invariant stationary PSF), the discrete type of the convolution is given by [46, 47],

$$g = h * f + v \tag{3.1}$$

where  $*$  represents the 2-D convolution operator and  $v$  represents additive noise. The frequency domain model obtained using the Fourier Transform is,

$$G = HF + V \tag{3.2}$$

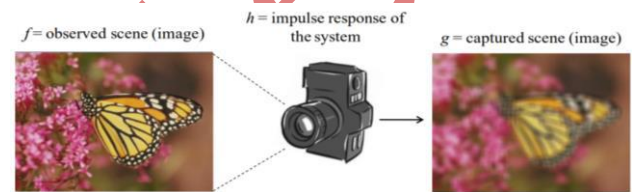


Fig.3.1 Image blurring model of a camera

The objective of deblurring is to deliver a decent estimation of the first picture  $f$ . This procedure is commonly known as convolution sifting or deconvolution [46] and deblurring on account of the rebuilding of obscured pictures.

In the commotion free case, having earlier learning of the PSF  $H$ , Eqn. 3.3 can be utilized to discover  $F'$ , an estimate of  $F$ , by,

$$F' = H^{-1} G \tag{3.3}$$

such that,

$$F' = F \tag{3.4}$$

This is known as opposite sifting [48]. On the off chance that the careful parameters for the tangling sign are known, it is sensibly expected that the first sign can be recouped precisely.

Likewise, if the Fourier change of the PSF contains zeros, the backwards separating turns into a poor reclamation strategy. This situation of deconvolution of the two sign when both are obscure is named 'blind deconvolution'. Stockham *et al.* in [49] were the first to coin the term for this problem.

#### Restoration Filters

The following section introduces the reader to some of the classical restoration filters that were used or studied in this research work.

**Inverse Filtering**

The most optimistic way to deal with deblur any picture is, evaluating the reverse of the PSF that obscured the picture and apply it to the obscured picture and recuperate the first picture. For a silent obscured picture case, the immediate reverse separating can without much of a stretch be connected in the ghastly (recurrence) space [48], since the convolution procedure will be changed over into increase. The inverse filtering procedure can be spoken to as:

$$F' = \frac{G}{H} \tag{3.8}$$

Much of the time the obscuring PSF isn't accessible particularly for genuine obscured pictures which prompts the genuine issues.

**Wiener Filtering**

As inverse filtering is very sensitive to additive noise which gets amplified during this process, a simple approach is to reduce single degradation at a time. The Wiener filtering is a estimating the image linearly. This is a stochastic framework based approach which can be given mathematically as:

$$F' = \left[ \frac{H^*}{|H|^2 + \delta} \right] \text{ where } \delta = \frac{|V|^2}{|F|^2} \tag{3.9}$$

The Wiener filtering executes an optimal trade off between inverse filtering and noise smoothing [61]. The additive noise is removed and so as the blurring is inverted simultaneously. The Wiener filtering is optimal in terms of the Mean Squared Error (MSE) [48].

**Iterative Blind Deconvolution Method**

IBD uses frequency domain by Fast Fourier Transform (FFT) and some of deterministic constraints in the form of non-negativity and finite support constraints. The algorithm is shown in Fig. 3.6 [29, 32, 62].

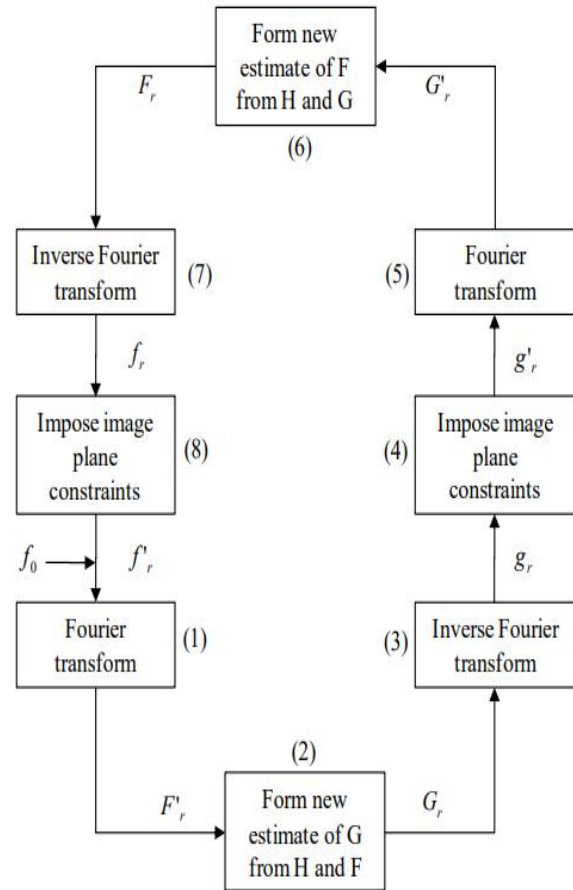


Fig 3.2 Block Diagram of Iterative Blind Deconvolution (IBD) algorithm

The IBD technique is well known due to its low intricacy [29, 32]. Another favorable position of this system is its strength to clamor which results from the poorly presented nature of the visually impaired picture deconvolution issue. In any case, the reverse channel is hard to characterize all over the place. IBD calculation additionally experiences questionable uniqueness, intermingling, precariousness and affectability to starting picture gauge [62].

**Richardson-Lucy Algorithm**

Richardson presented an iterative method of restoring degraded images in [27] based on Bays' theorem of conditional probability, by considering the image, PSF and degraded image probability functions. For an original image  $F$ , the PSF  $H$ , the degraded image presented by  $G$ , and the iteration  $k$ , Bays' theorem may be employed as follows

$$P(F|G_k) = \frac{P(G_k|F)P(F)}{\sum_{i,j} P(G_k|F)P(F)} \tag{3.10}$$

Also considering  $G_k$  with respect to its dependence on  $F$

$$P(F) = \sum_{i,j} P(F|G_k)P(G_k) \tag{3.11}$$

and

$$P(F|G_k) = P(F|G_k)/P(G_k) \tag{3.12}$$

Substituting Eqn. 3.10 in Eqn. 3.11, we get

$$P(F) = \sum_{i,j} \frac{P(G_k | F)P(F)}{\sum_{i,j} P(G_k | F)P(F)} P(G_k) \tag{3.13}$$

$$P(F) = P(F) \sum_k \frac{P(G_k | F)P(G_k)}{\sum_{i,j} P(G_k | F)P(F)} \tag{3.14}$$

The fundamental issue of blind Richardson-Lucy calculation is that it needs an underlying theory for the help size of blurring kernel. In spite of the fact that the blurring kernel is joined in the square circulate network structure, the help size must be either known or assessed, hence making the calculation non-blind.

**Regularization Based Deblurring Algorithm**

Investigating the convolution model of obscuring displayed in Eqn. 3.2, the picture gauge through opposite separating is given by Eqn. 3.15 as pursues

$$F' = \frac{G}{H} = F + \frac{V}{H} \tag{3.15}$$

The rebuilding error for this model is given by Eqn. 3.16

$$\|F' - F\| = \left\| \frac{V}{H} \right\| = \sqrt{\left\| \frac{V}{H} \right\|^2} \tag{3.16}$$

Because of the not well presented reverse issue, the reclamation mistake will take enormous qualities, especially enhancing the high recurrence clamor [64]. Because of this issue, the framework characterized in Eqn. 3.19 yields arrangements at focuses where the intensified high recurrence commotion veils the ideal arrangement *F*.

**Full-Reference IQMs**

For BID, quality measures have been created to assess the viability of individual plans or to assess diverse picture preparing calculations. In mistake based execution assessments, the reclamation is assessed by estimating the measure of progress in picture quality. To quantify that improvement, one needs the first, the twisted and the reestablished pictures accessible in the estimating procedure. Degree of rebuilding execution can by and

large be viewed as a procedure that takes in the first picture *f*, the mutilated picture *g* and the reestablished picture *f'* and restores a scalar worth. This yield worth is subsequently a measure to demonstrate how much the picture quality has been improved from the obscured picture *g* to the reestablished picture *f'* as for the first picture *f*. Recorded beneath are the variations of the mistake based execution measures, these measures are as yet utilized and in actuality most of the picture handling plans base their quality execution on these measures [81]. This is basically in light of the fact that these measures are anything but difficult to utilize and promptly give a numerical incentive to coordinate.

**Peak Signal to Noise Ratio (PSNR)**

Assessing deblurred picture quality requires a measure. MSE is an in all respects generally utilized quantitative measure in the sign and picture preparing network [48]. PSNR gives quantitative picture quality outcomes by scaling the MSE as indicated by the picture extend. For grayscale pictures with a pixel force run from 0 to 255, the PSNR is characterized as,

$$PSNR = -10 \log_{10} \left( \frac{\sum_{m=1}^N \sum_{n=1}^M (f(m,n) - g(m,n))^2}{255^2} \right) dB \tag{3.17}$$

PSNR is estimated in decibels (dBs). A higher estimation of PSNR speaks to a picture of high caliber. The PSNR isn't favored in light of the fact that the evaluated sign quality is taken as most extreme sign worth, instead of the genuine sign quality for the picture.

**Mean Structural SI Milarity Index (MSSIM)**

It measures the structural similarity between two images by comparing the intensiy patterns of locally pixels which are normalized for luminance and contrast. For two images *f* and *g* SSIM is given as.

$$S(f, g) = t(l(f, g), c(f, g), s(f, g)) \tag{3.18}$$

$$l(f, g) = \frac{2\mu_f \mu_g + C1}{\mu_f^2 + \mu_g^2 + C1} \tag{3.19}$$

$$c(f, g) = \frac{2\sigma_f \sigma_g + C2}{\sigma_f^2 + \sigma_g^2 + C2} \tag{3.20}$$

$$s(f, g) = \frac{\sigma_{fg} + C3}{\sigma_f \sigma_g + C3} \tag{3.21}$$

Where  $\mu$  = mean,  $\sigma$  = standard deviation of the images with constants  $C1, C2, C3$ . The major applications of SSIM are in denoising and classification [82, 83]. MSSIM must be higher in value to have higher quality of results.

**Universal Quality Index (UQI)**

It analyses the loss in correlation, luminance and contrast distortion keeping the base for quality among the two images. The UQI for two image signals  $f$  and  $g$  is defined in Eqn. 3.22 as,

$$Q(f, g) = \frac{4\sigma_{fg}\mu_f\mu_g}{(\sigma_f^2 + \sigma_g^2)(\mu_f^2 + \mu_g^2)} \tag{3.22}$$

Rearranging Eqn. 3.22 we obtain,

$$Q(f, g) = \frac{\sigma_{fg}}{\sigma_f \sigma_g} \cdot \frac{2\mu_f \mu_g}{\mu_f^2 + \mu_g^2} \cdot \frac{2\sigma_f \sigma_g}{\sigma_f^2 + \sigma_g^2} \tag{3.23}$$

The first term is the correlation coefficient of the two signals, whereas the secondhand third terms measure mean luminance and structural similarity. A higher estimation of UQI speaks to a picture of high caliber.

**Non-Reference IQMs**

IQMs have been high point of interest in image processing for blind evaluation of image quality. Two of the IQMs used in this research work are BRISQUE and NIQE. The other two IQMs, spatial and spectral kurtosis, are based on higher order data. Main advantage of such IQMs is that not only are they independent of reference image and features associated with distortion (i.e. ringing, noise, blur, or blocking). They have shown to compete well with top performing non-reference image quality analyzers trained on human judgments of known distorted images.

**Non-Gaussianity as a Quality Measure**

Conventional image performance measures work on the principle of subjective (qualitative) performance measures or quantitative quality measures which are based on error/difference image. These conventional measures, both subjective and error based, tend to have their own pros and cons. Even a combination of subjective and error based objective measures, like HVS based performance systems, fall short inapplicability, simply because of the very complex nature, limited knowledge and implementation difficulties of human eye behavior. These error based

techniques are dependent on relational matching between two images; the observed and the reference. Therefore, relational based performance evaluation techniques require reference image in addition to the observed and the restored image, which may not be available in any real life scenario, like digital camera photography. Hence, these performance indices cannot be used as a performance maximization criterion or act as a feedback parameter.

The obvious question of how it works can be answered as follows: the information content of a noise free and undistorted image is unique which does not remain the same when it is subjected to any degrading or distortion function. Hence, when any blurred image is treated by any deblurring algorithm, all it tries to do to bring the blurred image to its pristine form is to eradicate the distortions. From the perspective of the blurred image’s information content or the space of non-Gaussianity, this algo attempts to regain original information or to nonGaussianity, which otherwise happens to be at its minimum when it is blurred. Thus non-Gaussianity of the data can be employed as a performance measure, with or without the need of the original image as required by other measures, where it conserves as a feedback performance measure for the BID scheme. The quality index for comparing the performance of improvement/deterioration of any image can then be defined as,

$$Q_{NG} = \begin{cases} \frac{J_o}{J_1} & \text{if } J_1 \geq J_o \\ \frac{J_1}{J_o} & \text{otherwise} \end{cases} \tag{3.24}$$

Where,  $J_1$  and  $J_0$ , are non-Gaussianity of the original and the distorted image respectively. The advantage of using a non-Gaussianity based performance measure is not only that it works for both blind and non-blind situations, but also that it is robust against translational, orientation deviations etc.

Various measures can be used for computing the Gaussianity/non-Gaussianity of the image, with kurtosis and negentropy being the main ones used. Spatial domain nonGaussianity measures were used for blind image deblurring and denoising by Inland Husain in [86]. The measure and scheme based on it are defined in Section 3.9. Non-Gaussianity measure in the frequency domain, termed spectral non-Gaussianity measure, has been investigated in this research work as an alternate, more robust and computationally efficient IQM as compared to spatial kurtosis. The new frequency domain non-

Gaussianity IQM, spectral kurtosis, is presented in the research work illustrated in chapter 4.

### Blind/Reference-less Image Spatial Quality Evaluator (BRISQUE)

BRISQUE is a spatial domain natural scene statistic based distortion-generic nonreference IQM scheme. It utilizes the scene statistics of coefficients of locally normalized luminance to keep the “naturalness”. This model uses regression between features and quality. For a distorted image  $g$ , mean subtracted contrast normalized coefficient at each pixel is gained by,

$$\hat{g}(m, n) = \frac{g(m, n) - \mu_g(m, n)}{\sigma_g(m, n) + C}$$

(3.25)

with,

$$\mu_g(m, n) = \sum_{k=-U}^U \sum_{l=-V}^V w_{k,l} g_{k,l}(m, n)$$

(3.26)

$$\sigma_g(m, n) = \sqrt{\sum_{k=-U}^U \sum_{l=-V}^V w_{k,l} (g_{k,l}(m, n) - \mu_g(m, n))^2}$$

(3.27)

and  $C$  is a constant.  $w = \{w_{k,l} | k = -U, \dots, U, l = -V, \dots, V\}$  weighing function with  $U=V=3$ . Lower BRISQUE values are desired for higher quality of results.

### Natural Image Quality Evaluator (NIQE)

It is a completely non-reference quality analyzer that only makes use of measurable deviations from statistical regularities observed in natural images, without ground-truth, to provide quantitative comparisons. The model used for BRISQUE is also used for NIQE except there are some features of natural scene statistics used. The lower the NIQE, higher the image quality would be.

### Independent Component Analysis (ICA)

In view of Blind Signal Separation ICA is a method to uncover the unshown factors that basic arrangements of arbitrary factors, estimations, or sign. ICA characterizes a generative model for the watched multivariate information, which is regularly given as a huge database of tests.

### Maximum Non-Gaussianity Principle

Principle can be quoted as follows “Find the local maxima of non-Gaussianity of a linear combination  $y = \sum b_i x_i$  under

the constraint that the variance of  $y$  is constant. Each local maximum gives one independent component.” [36] Higher order cumulants have been used for BSS problem before [109]. Kurtosis, a fourth order cumulate, and negative entropy are two measures used in ICA to calculate the non-Gaussianity of a signal [73]

### Limitations of ICA

Although ICA-based schemes provide a framework to apply statistical independency concepts to blind deconvolution problems; their performance remains limited because of lack of observation samples, a prerequisite for BSS problems. Applying ICA on BSS or blind deconvolution problem requires fulfilling its pre-conditions, which essentially means providing as many observations as underlying sources and independency among all observations. Further, only one underlying source or observation can have a Gaussian distribution. As the convoluted signal is reverberate of its own adjacent samples or pixels (in case of an image) which are mixed as per the proportion defined by the PSF; thus resulting in single observation only. In order to have multi-channel representation as required by ICA, one has to resort to some alternate representation technique.

## IV. PROPOSED SYSTEM

### Introduction

A new possible substitute to the non-Gaussianity based deblurring measures is introduced in this chapter as the Blind Image Quality Measures (IQMs). In simulated blurring cases the pristine image and deblurred image can be used to calculate quality measures PSNR, MSSIM, etc. During BID, the source image is unavailable and an error image among the source and deblurred image cannot be calculated. This in turn leads to the impossibility of measuring the improvement in terms of error based or full-reference quality measures. It therefore raises the need to look for quality measures that can judge the deblurred image’s quality without the need for a reference pristine image, or in other words, a measure that does not require a reference. In this research work, the existing blind IQMs BRISQUE and NIQE have been investigated as alternate deblurring measures for BID. A novel full-reference yet blind quality measure is also proposed as IQM for blind deblurring.

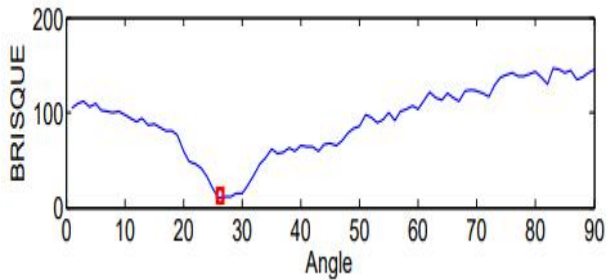
### BRISQUE and NIQE as Deblurring Measures

Both BRISQUE and NIQE does not require a reference image, it makes them good candidates by which to judge the quality of the deblurred image in BID. Using these measures, a deblurred image can be regarded as the best calculated approx. values of the original image at the point

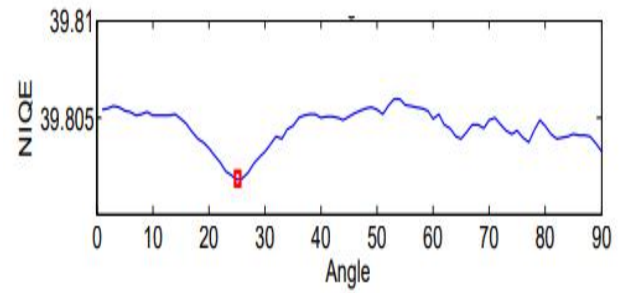
where the measurements are at minima. Figure 4.1(a) shows the deblurred image of the motion blurred (having blur PSF of length 11 pixels and angle 25 degrees) Barbara image. In figure 4.1(b) and (c) show the BRISQUE and NIQE plots are shown at different angles. Both these measures minimize in the near vicinity of the true blurring PSF parameters. The angles estimated by BRISQUE and NIQE are 26 and 25 degrees, respectively.



(a)



(b)



(c)

Fig.4.1 (a) An Image with Motion Blur (b) BRISQUE Plot (c) NIQE Plot

### Re-blurring Based Quality Measure for Blind Image Deblurring

An overview of the Re-blurring based BID techniques is shown in Fig. 4.2. The blurry image is given to the Restoring Filter to deblur and get image  $f'$  which is then re-convolved with PSF  $h$  to re-introduce blur in the image and obtain re-blurred image  $g'$ . A noise free restoration filter is desired to reproduce the same blur. To measure the similarity between the originally blur and re-blurred images, in this research, the PSNR measure has been utilized for comparison thus naming the proposed measure Re-blurring based PSNR (RPSNR).

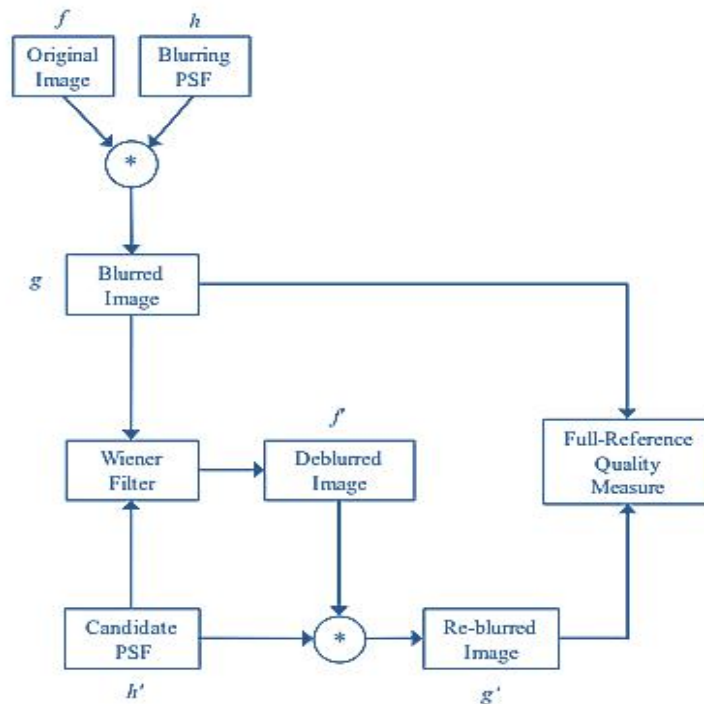


Fig.4.2. Schematic Diagram of the Re-blurring based BID Scheme

The deblurring result can be arranged into two unique situations. In the principal case, Wiener channel rebuilding is performed for an applicant channel like the first obscuring PSF. In the other situation where the Wiener channel is furnished with a competitor PSF not quite the same as the first obscuring PSF.

For instance, of the working of the plan, in Fig. 4.3 a unique picture obscured with movement obscure PSF at a point of 37 degrees, at that point deblurred picture is like the first picture with immaterial level commotion and ringing. The pictures acquired subsequent to deblurring were contaminated by clamor and ringing issues.

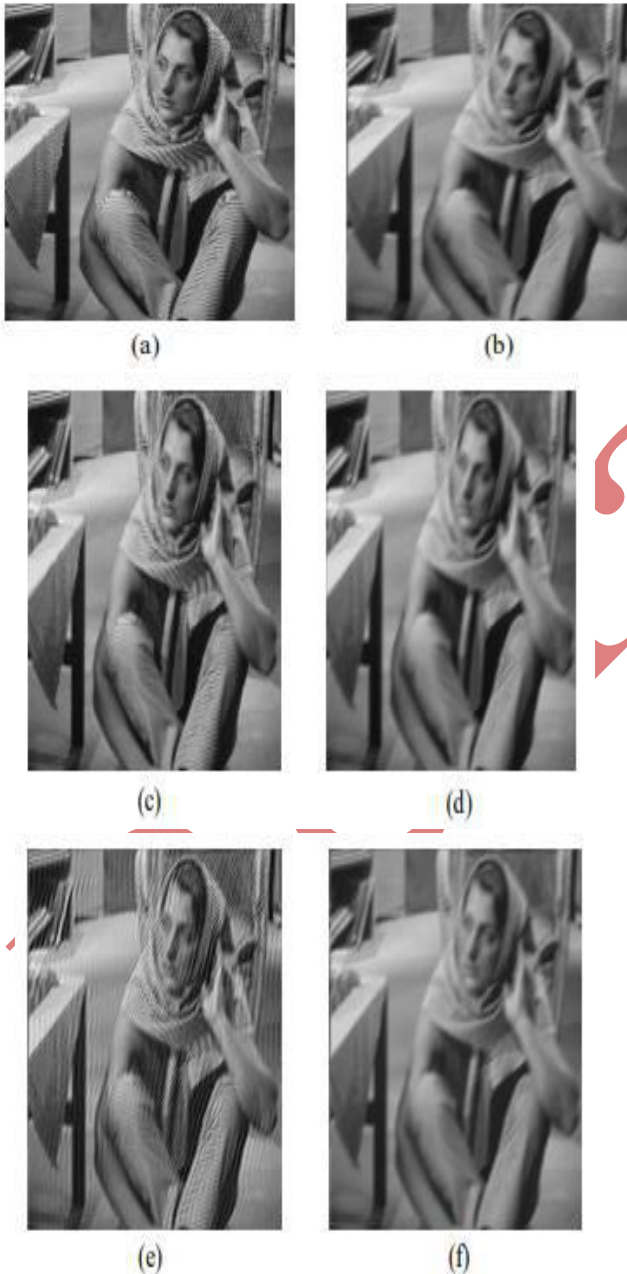


Fig. 4.3 (a) Original Image (b) Blurred Image (c)(e)(g) Images Deblurred with PSF angle 37, 16 and 52, with their respective Re-blurred Images in (d),(f) and (h)

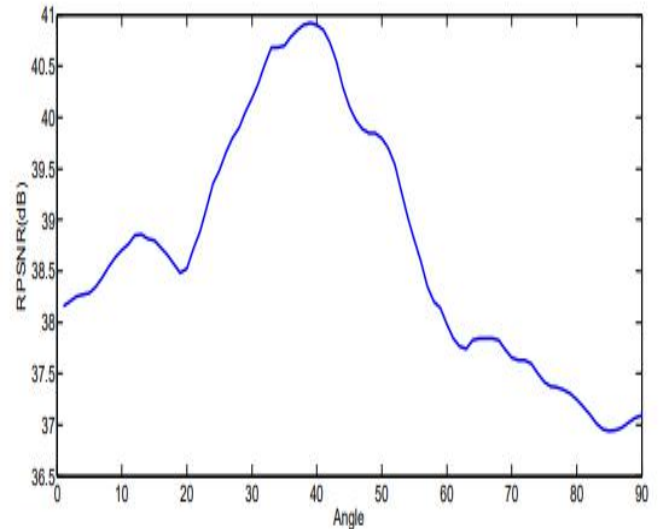


Fig. 4.4 RPSNR plot for Deblurring of Motion Blurred Barbara Image having PSF at angle 37 deg. The RPSNR Measure estimates the true blurring angle as 38 degrees at its maxima.

Fig. 4.4 shows the RPSNR plot for the deblurring of the blurred Barbara image in Fig. 4.3(b). The RPSNR measure during deblurring estimates the true blurring angle as 38 degrees at its maxima.

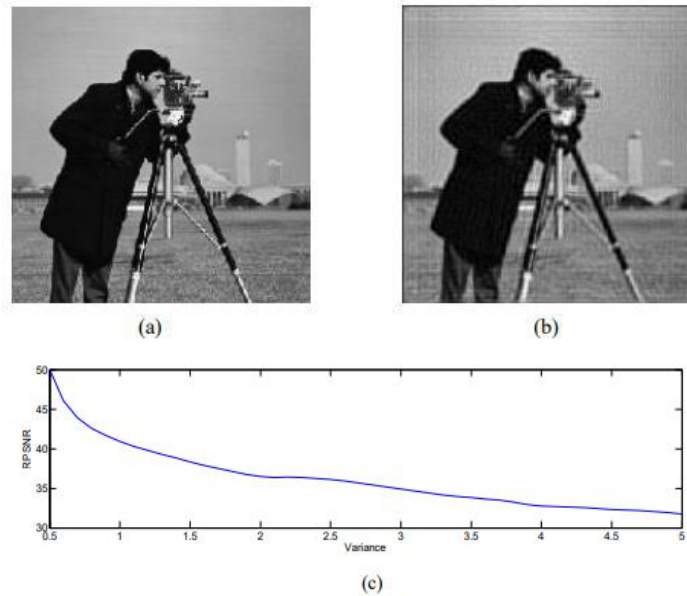


Fig.4.5 .RPSNR plot for deblurring of Gaussian Blurred Image with true blur variance of 2. The RPSNR measure incorrectly identifies the true blur variance as 0.5

The Re-blurring based BID scheme is limited to the deblurring of motion blurred images. The deblurring results for artificially blurred Gaussian and OF Images show that the RPSNR measure fails to depict a global

maximum value near the true blur parameters. Fig. 4.5 and Fig. 4.6 show the deblurring results in case of Gaussian and OOF blurred images.

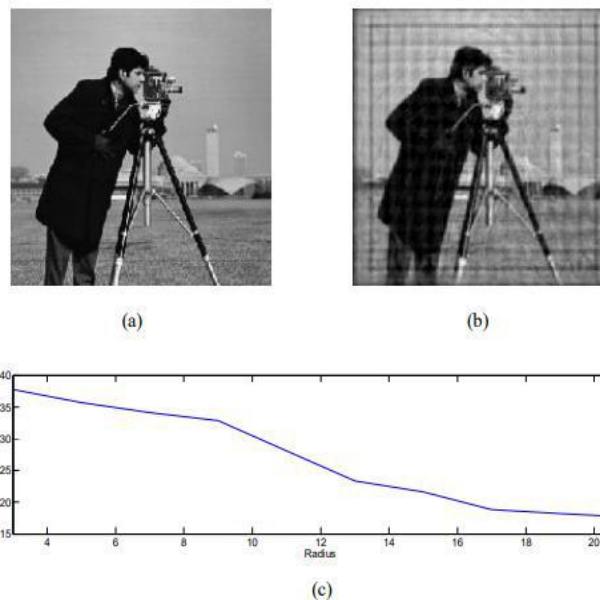


Fig. 4.6 RPSNR plot for deblurring of OOF blurred image with true blur radius of 11. The RPSNR measure incorrectly identifies the true blur radius as 1

### Deblurring Results for Artificially Blurred Images

Simulations were carried out to test the efficiency of the blind IQMs BRISQUE and NIQE and the full-reference blind IQM RPSNR. BRISQUE, NIQE and RPSNR have been tested as alternative deblurring measures. Experiments include testing of artificially blurred images as well as realistically blurred images. In the artificial

blurring cases, the three types of Parametric Blurs; i.e. Motion, OOF and Gaussian, have been considered. Fig. 4.7 shows the Cameraman image with blur at an angle of 35.35 degrees. The corresponding RPSNR, spatial and spectral kurtosis plots for deblurring are also shown. The RPSNR error measure estimated the angle as 32.5 degrees while spatial and spectral kurtosis estimated 32.25 as the

blur angle. Angle step size in this case was 0.25 degrees. This shows that the RPSNR measure maximizes in the

near vicinity of the true blurring parameter value.

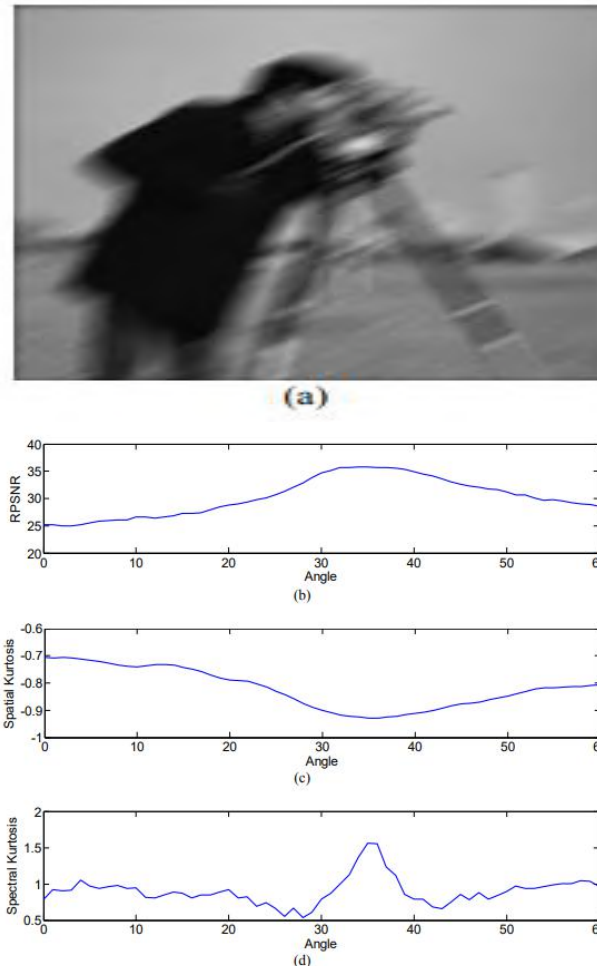


Fig.4.7 (a) Blurred Image (b) RPSNR Plot (c) Spatial Kurtosis, (d) Spectral Kurtosis Plot

Table 4.1 summarizes the RPSNR results for the artificially blurred Waterloo Bragzone images. In this case, motion blurred images were used and the blur angle, theta, was estimated. The estimated values are in close vicinity of the theta values used to blur the images. PSNR in

decibels (dBs) has been calculated for three set of images: blurred and re-blurred, original and blurred and original and deblurred. A higher value of PSNR shows image of high quality.

Table 4.1 PSNR comparison for the RPSNR based BID scheme

Figure	Original Theta	Calculated Theta	Blurred Reblurred PSNR (dB)	Original Blurred PSNR (dB)	Original Deblurred PSNR (dB)	Wiener-Filter NSR
Barbara	32.55	32	47.03	18.72	22.42	3.01e-03
Cameraman	47.45	46	40.84	15.29	24.41	4.01e-03
Goldhill	11.19	11.5	51.99	19.2	25.84	4.01e-04
Lena	111.21	110.5	44.82	19.74	26.09	3.01e-04
Mandrill	175.67	176.75	32.75	17.14	19.24	3.01e-04
Peppers	85.36	85.5	32.97	18.43	18.92	3.01e-04

**Deblurring Results for Realistically blurred Images**

Deblurring results of the blind IQMs for realistic images are given. In these, images under the effect of different types of blur including atmospheric blur, motion blur and

OOB blur are included. The results are compared to the spatial and spectral kurtosis-based estimates to gauge the efficacy of the deblurring measures. The estimated PSF are given in Table 4.2.

Table 4.2 Deblurring Results for Realistic Motion Blurred Images

Image	Estimated Values								
	Spatial Kurtosis			Spectral Kurtosis			BRISQUE		
	Length	Angle	SNR	Length	Angle	SNR	Length	Angle	SNR
Fig. 4.7 (a)	71	-2	4.01E-03	77	3	4.01E-02	71	0	4.01E-03
Fig. 4.8 (a)	19	80	4.01E-02	19	90	4.01E-02	15	81	4.01E-02
Fig. 4.9 (a)	16	161	4.01E-03	21	160	4.01E-03	20	161	4.01E-03

Image	Estimated Values					
	NIQE			RPSNR		
	Length	Angle	SNR	Length	Angle	SNR
Fig. 4.7 (a)	73	3	4.01E-03	77	3	4.01E-03
Fig. 4.8 (a)	17	87	4.01E-03	19	80	4.01E-02
Fig. 4.9 (a)	17	156	4.01E-03	21	156	4.01E-03

In Figure 4.8 (a), an image with motion blur shows unreadable text. An ordinary digital camera clicked this image with person in motion while being clicked. The image in Fig. 4.8(b), (d) and (e) seem to have recovered well by deblurred with PSF estimated using the spatial

kurtosis, RPSNR and BRISQUE based BID schemes, respectively. In the case of spectral kurtosis and NIQE based BID scheme, the images in Fig. 4.8(c) and Fig. 4.8(f) do not recover well.

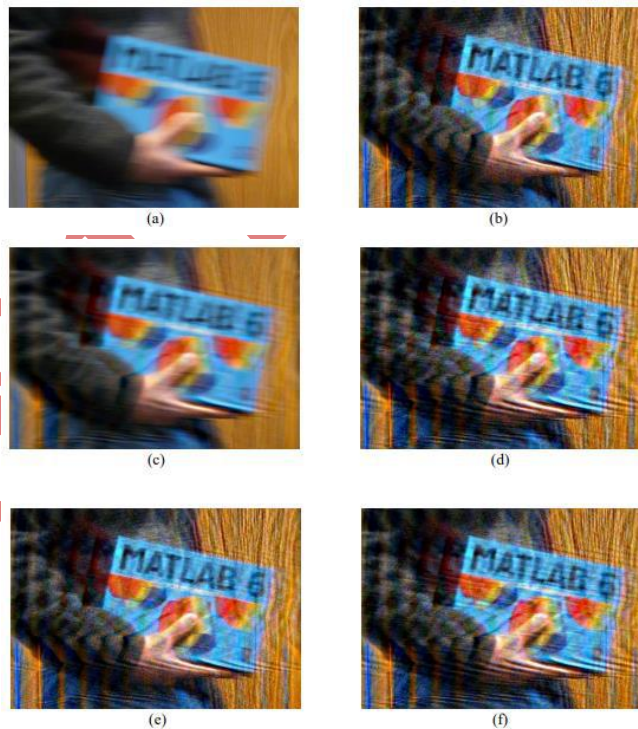


Fig.4.8 (a) Blurred Image (b) Spatial Kurtosis Measure (c) Spectral Kurtosis Measure. (d) RPSNR Measure (e) BRISQUE Measure (f) NIQE Measure based BID scheme

**Proposed BID Scheme for Arbitrarily Shaped PSF Estimation**

A PSF can be assumed as an array of random values under the constraints mentioned below:

- The PSF has certain row ( $m$ ) and columns ( $n$ ) with the finite support size.
- The energy of the PSF is maintained i.e.  $\sum h(m, n) = 1$
- The PSF is space invariant. The same blurring/averaging effect is presented by the blurring kernel at each pixel location.
- The PSF coefficients are non-negative.

During each iteration, a coefficient value is updated in the direction of improved deblurred image quality which can be calculated using any restoration measure e.g. spatial or

spectral non-Gaussianity measures, non-reference or full-reference IQMs etc. The process can be evaluated for a fixed number of iterations or it can be terminated when the difference in the measure value in subsequent iterations is lower than a specified threshold value.

Fig. 4.9 shows a glimpse of the restoration process by estimating the PSF coefficients. The original PSF is depicted in Fig. 4.9 (a) while the estimation process is illustrated in Fig. 4.9 (b). From an initial set of random values, the process keeps on estimating/changing the PSF weights till the deblurring measure stops showing improvement.

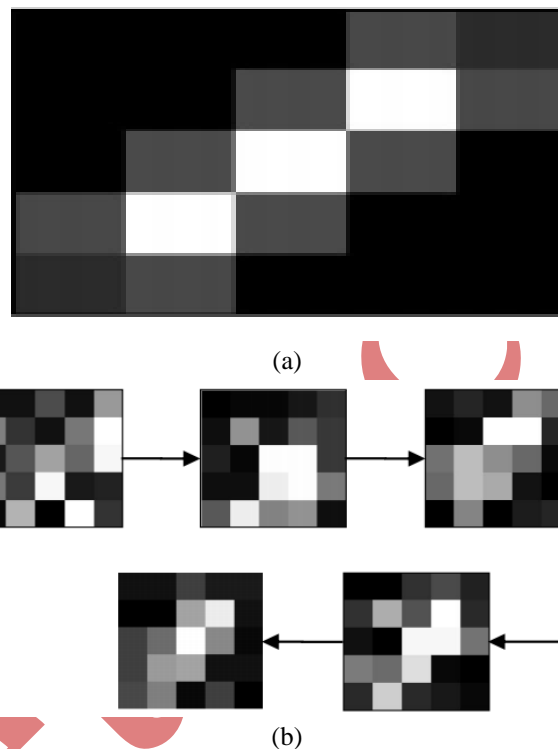


Fig.4.9 (a) Blurring PSF (b) PSF Estimation Process through different steps

The deblurring scheme is optimized using GA. An added advantage of such a BID scheme is that the same method can easily be extended for estimating other types of blur apart from camera handshake. Also, the BID scheme based on GA is flexible and so it can be easily incorporated with any deblurring measure as the fitness function. Details of the GA based optimization are as follows:

- Step 1: Initiate the GA process with population, crossover rate, size, mutation rate etc.
- Step 2: Generate an initial chromosome population where each chromosome contains information about all the coefficients of the finite support size PSF.
- Step 3: Iterate, find the restored image through Wiener filtering for all the chromosomes.

- Step 4: Calculate fitness function values for the initial population.
- Step 5: Select the best fitting group of chromosomes based on either roulette or Threshold based selection.
- Step 6: Generate a new population from the chromosomes selected in Step 5 through crossover and mutation. Each crossover is performed with probability  $p_c$  {0.5-0.8} and cross over points are selected at random. Mutation involves modification of components of the individual chromosomes with probability  $p_m$  {0.001-0.01}. Roulette wheel selection is used to select the best fitting individuals among the populations.

- Step 7: Keep the process repeat from 3<sup>rd</sup>Step till it converges for the deblurring measure.

### Deblurring Results for Artificially Blurred Images

Since the BID scheme can also be extended for uniform parametric blurs, the algorithm was first evaluated for the less complex parametric form blurs before testing it for arbitrarily shaped PSFs. Results of deblurring the Gaussian, motion and OOFPSF based blur are presented below.

### Restoration of Parametric PSF Blurred Images

The first set of tests included deblurring images blurred by Gaussian PSF. Results of deblurring for Gaussian PSF blurred images is shown in Fig. 4.10. It can be observed that the estimated PSF takes on a rough shape of the blurring PSF as viewed in Fig. 4.10(e). Results presented here were obtained when the algorithm stopped, as the tolerance value for the fitness function was attained. The restored image appears sharper and much more detailed than its blurred counterpart.

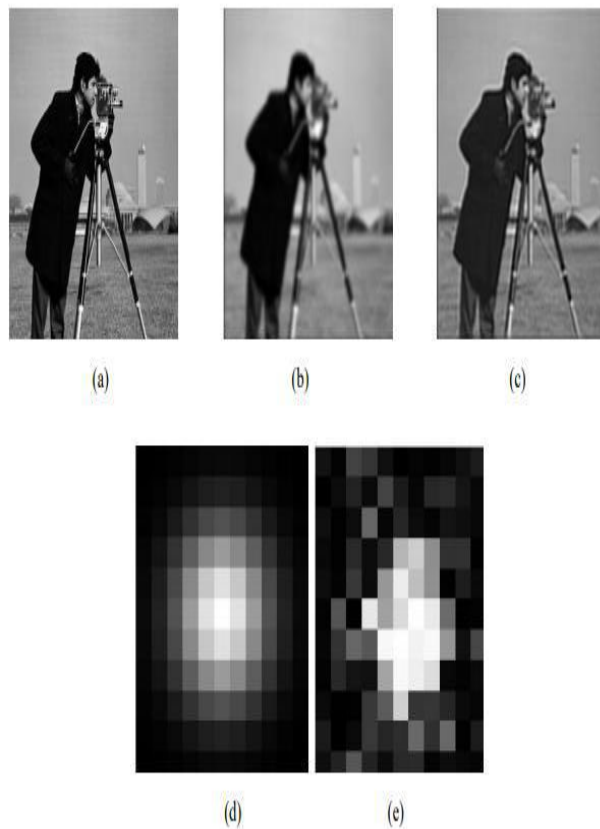


Fig.4.10 Deblurring Result for Image Blurred by Gaussian PSF of Size  $11 \times 11$  Pixels and Variance  $\sigma^2 = 2$ . (a) Original Image (b) Blurred Image (c) Deblurred Image (d) Blurring PSF and (e) Estimated PSF

The second set of tests included deblurring images artificially blurred by motion blur. Fig. 4.11 shows such case. And Fig. 4.12 shows the results of deblurring for Barbara images under the influence of OOF blur with the radius of 9 pixels. Deblurring results show the estimated

PSF converging towards the original blur PSF. For large OOF blur, a lot of attenuation occurs for the high frequency elements in the image and recovery in this case is not that sharp as observed for the Barbara image in below figure (c)

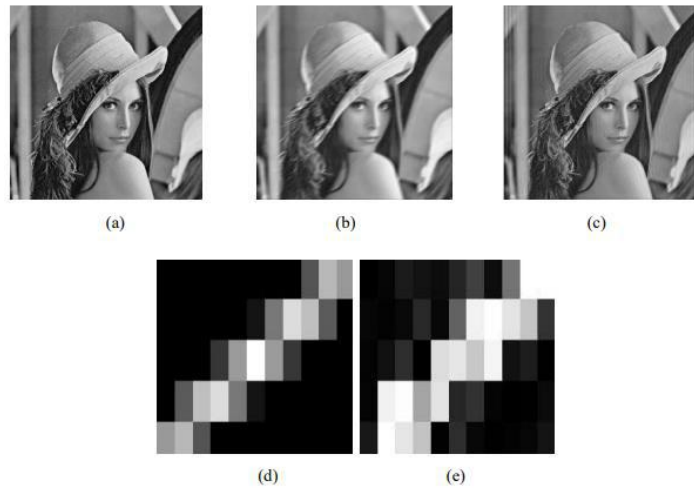


Fig.4.11 Deblurring result for image blurred by the Motion Blur PSF with length of 11 pixels and the angle as  $23^\circ$ . (a) Original, (b) Blurred, (c) Deblurred, (d) Blurring PSF and (e) Estimated PSF

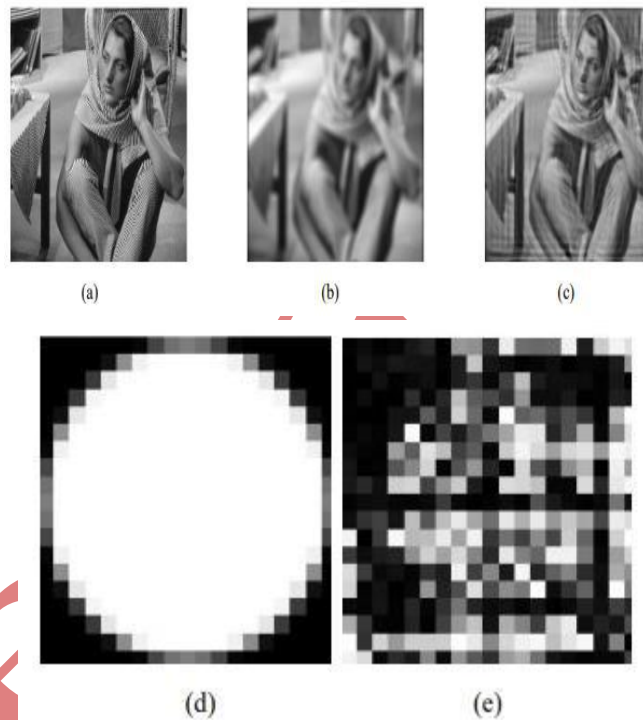


Fig.4.12 Deblurring Result for Image Blurred by OF Blur PSF with Radius of 9 Pixels. (a) Original (b) Blurred (c) Deblurred (d) Blurring PSF and (e) Estimated PSF

### Deblurring Images Blurred by Arbitrarily Shaped PSFs

Arbitrarily shaped PSFs were used to blur the images and then recover using the proposed scheme. Deblurring

results shown in figures depict that the proposed algorithm was able to estimate the blurring shape/coefficients to a great extent. The deblurred images appear sharper than their blurred counterparts.

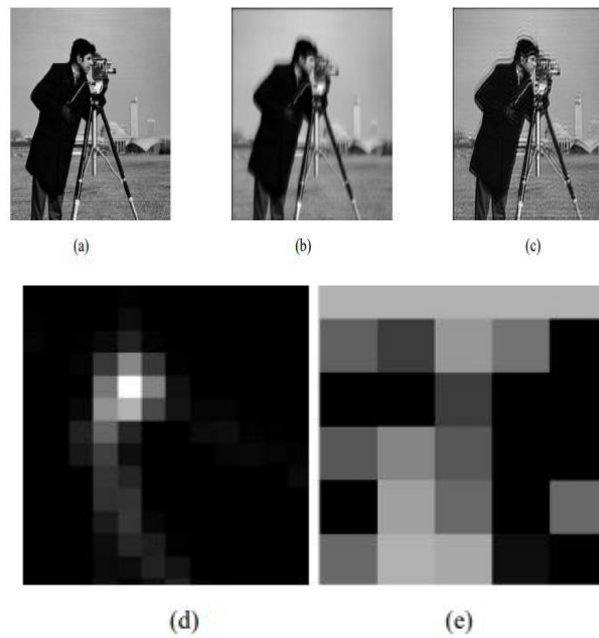


Fig. 4.13 Deblurring result for Cameraman Image blurred by arbitrary PSF of size 15 x 11 pixels. (a) Original, (b) Blurred, (c) Deblurred, (d) Blurring PSF and (e) Estimated PSF

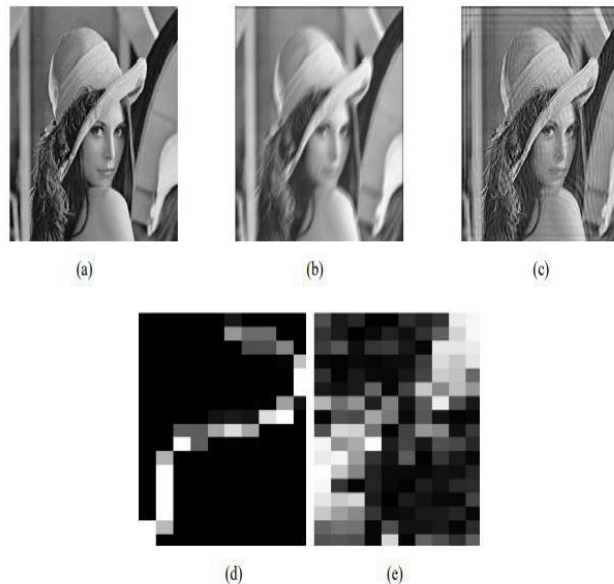


Fig.4.14 Deblurring result for Lena image blurred by arbitrary PSF of size 16 x 10 pixels. (a) Original, (b) Blurred (c) Deblurred, (d) Blurring PSF and (e) Estimated PSF.

Table 4.3 illustrates the IQMs values for the images deblurred using the arbitrarily shaped PSF estimation scheme.

Table 4.3 Deblurring results for artificially blurred images. Deblurred image quality is evaluated using BRISQUE and NIQE IQMs

Figure Name	Blurring Filter	Size (Pixels)	Parameter Value	Image Quality Measured using BRISQUE			Image Quality Measured using NIQE		
				Original	Blurred	Deblurred	Original	Blurred	Deblurred
Fig 4.10	Gauss.	11x11	Var = 2.0	6.68	35.88	47.27	5.11	4.57	6.89
Fig	Motion	5x11	L=11, A=23	10.26	16.67	52.07	5.11	4.69	7.19

4.11									
Fig 4.12	Out of Focus	19x19	R=9	50.12	30.57	63.38	4.98	6.12	9.66
Fig 4.13	Arb.	15x11	-	14.13	17.95	36.43	5.50	5.94	7.56
Fig 4.14	Arb.	16x10	-	15.45	20.77	49.80	4.98	5.72	6.30

## V. IMPLEMENTED MODEL

### Introduction

A GUI enables the user to easily access and use software. It can save valuable time and avoid trouble by evaluating user desired function through a platform of function button and other easy access tools. The lack of GUI results in creating unnecessary difficulty for the user to operate the BID scheme. Most of the BID schemes visited in the literature that result from scientific research usually lack a GUI and are thus not available in the form of toolboxes or individual software. Some of the major reasons are as follows:

- BID algorithms may not be completely automated because of their dependency on such human intervention at different stage(s) of deblurring that cannot be covered by the GUI tools. In such cases multiple files of codes are rather utilized to perform the BID in multiple stages manually by obtaining result from one code file and putting it in another code file as in the case of Shan et al. [39] BID scheme.
- Most of the BID schemes usually address a limited range of the deblurring 128 problems i.e. either dealing with parametric or non-parametric blur, space invariant or variant blur etc. GUI development in such case would only be useful for limited users.
- BID schemes may not be computationally efficient or they may require further modifications to enhance their deblurring results and thus incorporating them in form of GUI at early stages is not desired.

The benchmark BID schemes (Shan et al. [39], Fergus et al. [17] and Whyte et al. [18]) used for comparison in this research work also lack a graphical interface. Shan et al.'s BID scheme requires command line input to Windows batch files and lacks GUI. The user has to input different parameter values to the batch file required to conduct BID on the image. Fergus et al. and Whyte et al. BID schemes use MATLAB code and require user interaction in image loading, parameter setting in code files to deblurring result presentation. Recently presented BID schemes

In this research, a GUI Model for non-blind image deblurring was developed during the early stages and was regularly updated to incorporate many additional features including region based deblurring, blind IQMs for BID and parametric and nonparametric PSF estimation. After the successful use of blind IQMs for BID, the toolbox was updated to incorporate a GA based BID scheme which can use any of the blind IQMs as a fitness function. It can estimate parametric and arbitrarily shaped PSFs as well.

### Key Features of Implemented Model

The toolbox and the related GUI have features incorporated which allow for:

- Deblurring the complete image or section of it. A moveable bounding box is provided for the user to select any or whole region of the image to deblur as shown in Fig. 5.1 and Fig. 5.2.
- Deblurring with different restoration filters: Wiener, Richardson-Lucy and Regularized. The user can select among any of these classical restoration filters and update their parameter settings.
- Sliders for setting values for PSF parameter(s) in the case of non-blind deconvolution.
- Deblurring different types of blurs, Gaussian, motion and autofocus blur.
- Setting values for PSF parameters, e.g. PSF size and variance for Gaussian blur, and radius for autofocus blur, length and angle for motion blur for non-blind deconvolution. The parameter values can be set manually.
- Ringing reduction by using edge-taping technique applied to the image prior to deblurring. This feature is embedded in the code and is always applied to the image.
- File loading and saving and layout change. Image file can be loaded for BID and the deblurred result can be saved using a Windows based file explorer.
- The GUI can execute the code in either serial or parallel mode as desired by the user.

- The GUI allows for easy modification and amendment of the features.

The model is built using MATLAB and its GUI implementation framework named GUIDE as it allows for an easy creation and updating of the GUI. GUIDE based GUI is coded by separate function allowing for easy access and incorporation of future updates. The MATLAB based GUI also supports parallel processing by simply using its distributed computing techniques. The following sections discuss briefly the design and implementation of the toolbox.

### Model Design

The flowchart for the toolbox is presented in Fig. 5.1 shows the workflow of the Model. The Model's functionality can be divided into three main parts: the data input, BID algorithm execution and the deblurring output section.

### Data Input

The toolbox takes the image file in three common image formats at the moment i.e. JPEG, TIFF and PNG. Other formats are also available as optional to the user. After the GUI loads, the user can load an image file by browsing through the computer directory and locating the image file as shown in Fig. 5.2. Once the image is loaded, the user can relocate the bounding box that selects the image section as shown in Fig. 5.3. By default, it covers the whole image.

The user then needs to specify the initial PSF size used for estimation. The user can also select among different deblurring filters i.e. Wiener, Richardson-Lucy and Regularized filter as shown in Fig. 5.4. Settings of the filter need also be input e.g. NSR for Wiener filter, number of iterations for Richardson-Lucy filter etc.

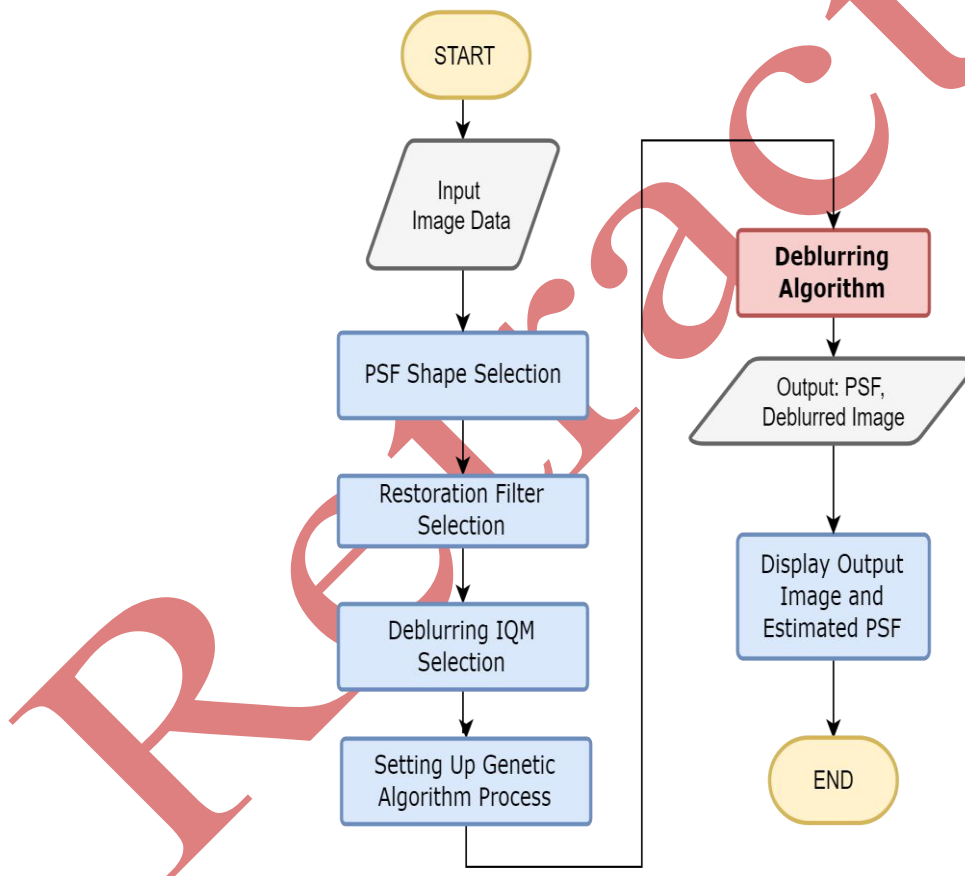


Fig.5.1 Flowchart presenting the BID Model Implementation

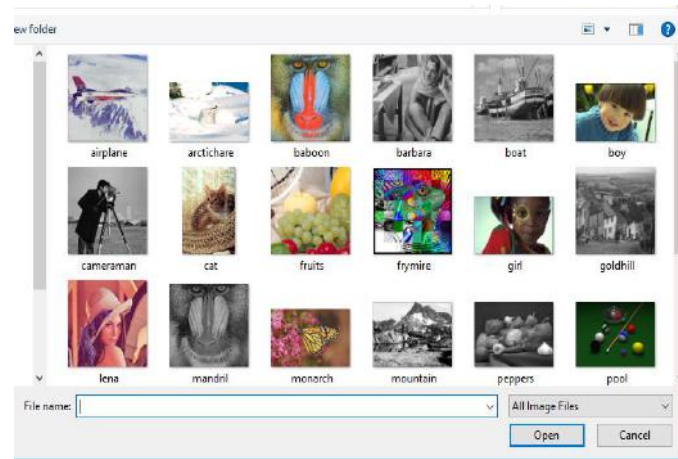


Fig5.2. The image loading window available in the BID Model for Selecting an Image

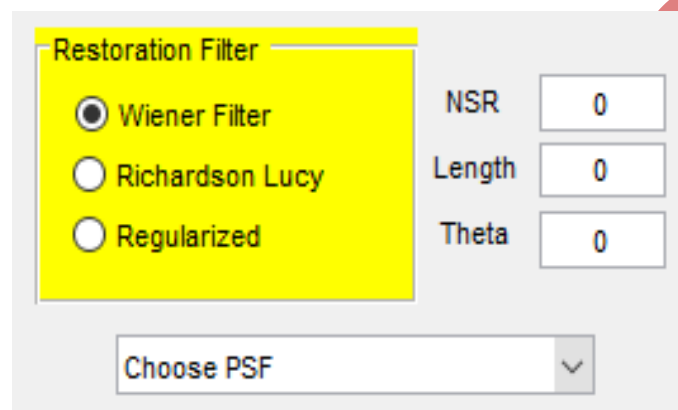


Fig.5.3 Different Filters available for BID in the GUI Model

The user has the choice of selecting among different IQMs as fitness function for the GA. List of the IQMs is given in Fig. 5.5.

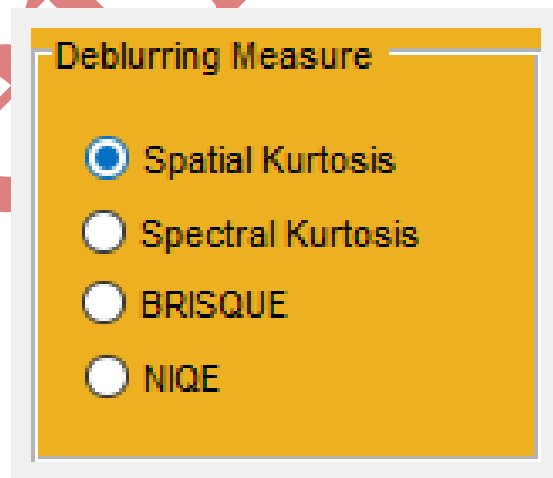


Fig.5.4 Different Deblurring Measures for BID in the GUI Model

The GA settings need to input by the user as well, if not the default values for number of iterations, initial population size, fitness function tolerance etc. are used. Advanced settings of the algorithm include parameter tuning for mutation rate, crossover rate, parallel processing etc. The setup screen is shown in Fig. 5.5.

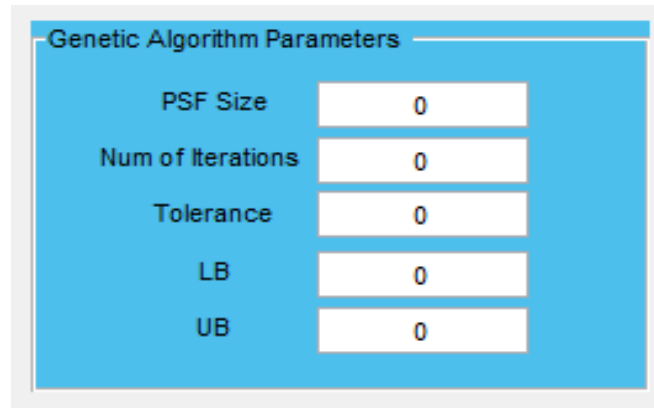


Fig. 5.5 GA Setup Screen for BID in the GUI Model

### Deblurring Output

Fig. 5.6 shows an overview of the GUI Model where the complete image is deblurred. The picture has been deblurred using a motion blur PSF and angle 0 degrees using a Wiener filter.

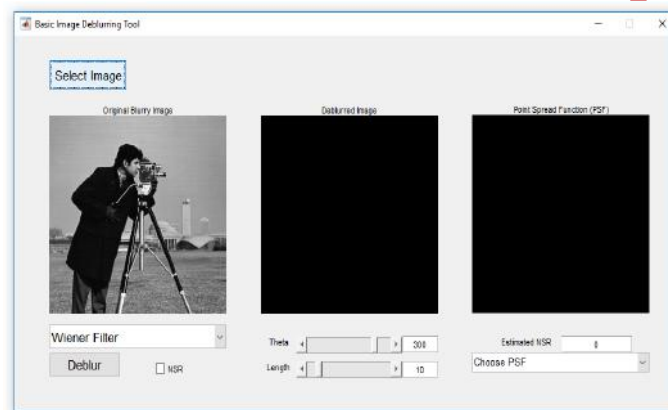


Fig. 5.6 BID Model for Non-Blind Image Deblurring.

Fig. 5.7 shows the latest GUI for the BID Model which allows for the estimation of arbitrarily shaped PSFs. It also has features to load the blurred image and save the deblurred image. Other different options are also available in the main menu. The toolbox allows the user to select from different restoration filters and provides easy access to their settings. The deblurring algorithm is optimized through GA. The GA parameters can be set up simply. The deblurring algorithm can be optimized on a multiple core machine as well. The user can select from four deblurring

measures as the fitness function for the GA. These deblurring measures are spatial and spectral kurtosis, RPSNR, BRISQUE and NIQE. By using the proposed Blind Image Deblurring Model in Section 5.2, GA aims to estimate the PSF coefficient values for a coefficient matrix whose size has to be input by the user. This toolbox therefore provides a single base to tackle the BID problem for images blurred by parametric and arbitrarily shaped PSFs using any of the deblurred measures.

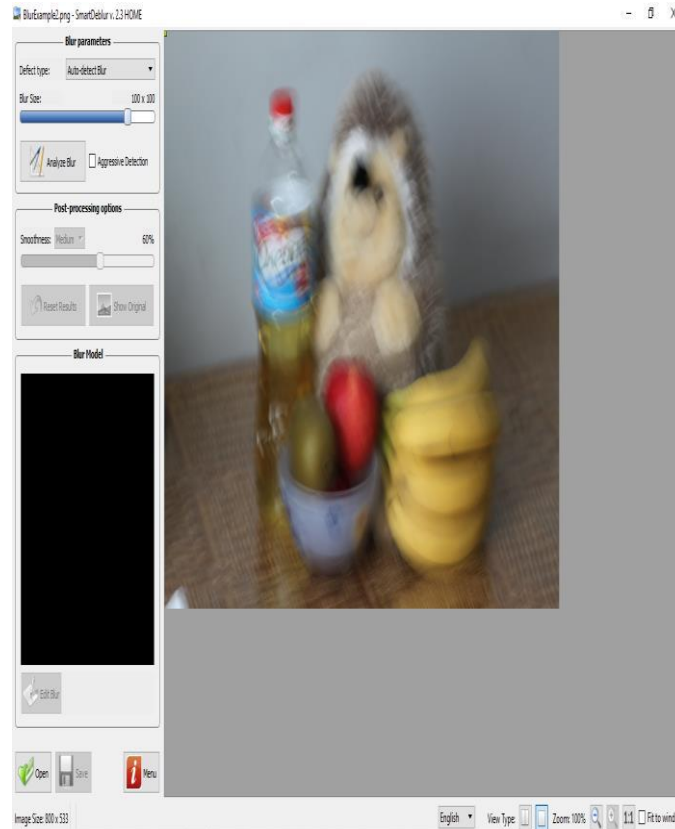


Fig. 5.7 GUI Model for blind PSF estimation and Image Deblurring

### Comparison with Other BID Models

Other BID toolboxes are available and their functionality is discussed in comparison to the proposed BID scheme's GUI. This includes the Smart Deblur Toolbox. The toolbox allows for manual deblurring of out-of-focus and motion blurred images. The user has to manually adjust the blur parameters and search for the best

parameter values to deblur the image. It allows the user to adjust motion blur length and angle parameter and radius parameter of out-of-focus blur. The smoothness parameter allows the user the level of deblurring residual blur and the correction strength allows the level of deblurring to be applied on the **blur image**.

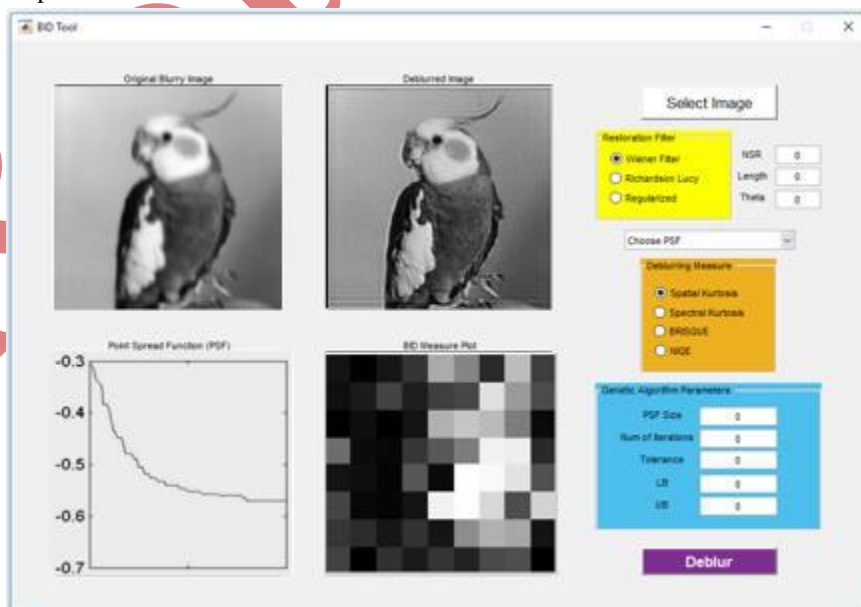


Fig. 5.8 Smart Deblur BID Toolbox for Manual Deblurring

## VI. CONCLUSION

This research was an investigation to establish that the blind image deconvolution problem can be solved to a fair degree of complexity by using the information theoretic concept, where, an independent signal has certain useful information. The focus was carried out on issues of BID (i.e. design and implementation of a robust BID Measure, estimation of PSFs and definitely deblurring of blurred images with enhanced efficiency and quality), and finding a solution.

Blind IQMs were investigated as feedback deblurring measures to the BID. These include; spatial kurtosis, spectral kurtosis, RPSNR, BRISQUE and NIQE index. Spatial kurtosis has been previously used for BID while existing measures, BRISQUE, NIQE and spectral kurtosis taken as deblurring measures for BID. A novel full reference yet blind IQM, RPSNR designed and used in this research work.

Starting with the spatial kurtosis-based BID scheme as a reference, the spectral kurtosis-based BID model was designed and implemented. Some of the features of this scheme are as follows:

- Since the spectral kurtosis measure is calculated in the frequency domain thus limiting the need for Inverse Fourier Transform which is required for the calculation of spatial domain IQMs (spatial kurtosis, RPSNR, BRISQUE and NIQE). This makes spectral kurtosis computationally efficient. However, MATLAB's Wiener filter implementation also has other severe overheads losing the per iteration efficiency.
- Spectral kurtosis maximizes for increased blurring unlike spatial kurtosis which increases and decreases for sub-Gaussian and super-Gaussian image. This makes the BID scheme based on spectral kurtosis easily automatable.
- Experiments were carried out on a number of test images with various blurring parameters. Spectral kurtosis-based BID scheme is robust as it is able to estimate the blurring parameters over a wide range of images and its performance is not marred by ringing artifacts and inherent deblurring noise in the images.
- The proposed method's deblurring ability is not limited to a single blurring function. The algorithms and gradients are derived for a number of blurs, and the performance improvements are corroborated through a set of simulations. The benefit of using such a model of estimation is that it makes the same BID algorithm easily tunable, allowing it to estimate any of the mentioned parametric blur types using the same IQM.

- A Gradient Descent based scheme was utilized where the parameter(s) of the blur model were worked to optimize and maximizing the spectral non-Gaussianity. The BID scheme was later replaced by the use of a GA based optimization. The GA based BID scheme was used for testing of RPSNR, BRISQUE and NIQE measure as well.

A novel full-reference yet blind quality measure for BID, RPSNR, was designed as an alternative to the spectral kurtosis measure.

- Reference based error computing was not previously possible in BID cases, due to the unavailability of a reference image required for comparison purposes. The RPSNR measure suggests a solution to this problem by calculating error between blurred and reblurred image.
- Deblurring results for artificial and natural (real) motion blurred images based on the RPSNR based BID techniques are encouraging. However, the measure's performance was limited for Gaussian and out-of-focus images.

Non-reference IQMs BRISQUE and NIQE were investigated as deblurring measures alternate to the spatial and spectral non-Gaussianity measures.

- BRISQUE measure based PSF estimates depict better results for deblurring of artificially and real-life blurred images as compared to other IQMs.
- From detailed testing of these measures with deblurring experimentation on the artificial and real-life blurred images, BRISQUE proved to be a very robust but computationally costly PSF estimator. BRISQUE is computationally costly due to its usage of a support vector machine for calculating the image quality.
- BRISQUE based BID estimates PSF for relatively lower NSR values as compared to other IQMs resulting in a comparatively sharper image with presence of deblurring noise.

All the deblurring measures show absolute maxima at the true PSF parameter values except the spatial kurtosis measure, which maximizes for super-Gaussian images and minimizes for sub-Gaussian images. This makes them a better choice in terms of an automatable measure.

In the earlier research work, parametric forms of blurs were used to model the blurring in the images. The IQMs were used to successfully tackle parametric blurs for both artificial and natural (real) blurred images. The parametric model is a mere approximation of the blurring that occurs in real life blurred images. The research study was further extended to focus on the estimation of the arbitrarily shaped

PSFs that present much more complex forms than their parametric counterparts.

- A GA based novel BID scheme using BRISQUE measure as the fitness function was used to calculate the factors or coefficients of the arbitrarily shaped PSFs.
- The BID scheme's setup allows for the estimation of any type of PSF i.e. atmospheric turbulence blur (through Gaussian approximation), motion blurs, and out-of-focus blur in parametric form with arbitrarily shaped as well. The BID scheme was also utilized for parametric blur estimation as well.
- The proposed BID scheme's estimated PSF coefficients are not exactly the same as the original PSF but are rather a near approximation to the original PSF for blur. This BID technique estimates the PSF coefficients for limited number of iterations which produces a reasonable approximation of the original PSF coefficients.
- The proposed BID scheme requires a fixed PSF size input from the user. In order to estimate the PSF support size, a simple technique based on visual judgment of ringing artifacts in the deblurred image is proposed
- Experimentation with artificially blurred images, for parametric and arbitrarily shaped PSF, depicts excellent restoration results. However, the deblurring capability was not satisfactory when tested on real life blurred images corrupted by arbitrarily shaped PSFs and in presence of a low degree of noise.
- Other benchmark schemes used for comparison also failed to produce any viable result as they were not able to estimate the right PSF shape/coefficients.
- Full reference and non-reference IQMs taken up to measure the quality of reconstructed image after deblurring an artificially blurred image.
- The MATLAB based GUI also supports parallel processing by simply using its distributed computing techniques.

## REFERENCES

- [1] Chengtao Cai, An Lui, Baolu Zhang, Motion Deblurring from a Single Image, 2016 IEEE 20<sup>th</sup> International Conference on Computer Supported Cooperative Work in Design
- [2] Xu Y, Hu X, Peng S. "Blind motion deblurring using optical flow," *Optik-International Journal for Light and Electron Optics*, vol. 126, no. 1, pp.87-94, 2015
- [3] F.Alaoui, A. Ghlaifan Abdo Saleh, V.Dembele, A.Nassim, Application of Blind Deblurring Algorithm for Face Biometric, *International Journal of Computer Applications* (0975 – 8887)Volume 105 – No. 2, November 2014
- [4] C. Y. Zhou, S. Lin, and S. K. Nayar, —Coded Aperture Pairs for Depth from Defocus and Defocus Deblurring, *International Journal of Computer Vision*, vol. 93, no. 1, pp. 53-72, May, 2011.
- [5] Aftab Khan, Hujun Yin, —Parametric blind image deblurring with gradient based spectral kurtosis maximization *International Society for Stereo logy & Image Analysis*, DOI: [10.5566/ias.1887](https://doi.org/10.5566/ias.1887), 2018.
- [6] A. Veeraraghavan et al., —Dappled Photography: Mask Enhanced Cameras for Heterodyned Light Fields and Coded Aperture Refocusing, *ACM Transactions on Graphics*, vol. 26, no. 3, July, 2007.
- [7] R. Raskar, A. Agrawal, and J. Tumblin, —Coded Exposure Photography: Motion Deblurring Using Fluttered Shutter, *ACM Transactions on Graphics*, vol. 25, no. 3, pp. 795-804, July, 2006.
- [8] S. Hiura, and T. Matsuyama, "Depth Measurement by the Multi-Focus Camera," *Proceedings of IEEE Computer Society Conference on Computer Vision and Pattern Recognition*. pp.953-959.
- [9] M. Ben-Ezra, and S. K. Nayar, —Motion-Based Motion Deblurring, *IEEE Transactions on Pattern Analysis and Machine Intelligence*, vol. 26, no. 6, pp. 689-698, Jun, 2004.
- [10] E. Lopez-Rubio, R. M. Luque-Baena, and E. Dominguez, —Foreground Detection in Video Sequences with Probabilistic Self-Organizing Maps, *International Journal of Neural Systems*, vol. 21, no. 3, pp. 225-246, Jun, 2011.
- [11] D. L. Li, and S. Simske, —Atmospheric Turbulence Degraded-Image Restoration by Kurtosis Minimization, *IEEE Geoscience and Remote Sensing Letters*, vol. 6, no. 2, pp. 244-247, Apr, 2009.
- [12] R. Cruz-Barbosa, and A. Vellido, —Semi-Supervised Analysis of Human Brain Tumours from Partially Labelled MRS Information, Using Manifold Learning Models, *International Journal of Neural Systems*, vol. 21, no. 1, pp. 17-29, Feb, 2011.
- [13] G. H. Glover, —Deconvolution of Impulse Response in Event-related BOLD 153 fMRI, *Neuroimage*, vol. 9, no. 4, pp. 416-429, Apr, 1999.
- [14] T. Taxt, and J. Strand, —Two-Dimensional Noise-Robust Blind Deconvolution of Ultrasound Images, *IEEE Transactions on Ultrasonics Ferroelectrics and Frequency Control*, vol. 48, no. 4, pp. 861-866, Jul, 2001.
- [15] L. I. Shi, Z. Bao, and S. U. N. Hui, —Restoration of Aerial Multiple Blurred Images, *Optics and Precision Engineering*, vol. 17, no. 5, pp. 1161-1170, 2009.
- [16] W. Jun, and C. Danqing, —Deblurring Texture Extraction from Digital Aerial Image by Reforming a Steep Edge Curve, *Geo-spatial Information Science*, vol. 8, no. 1, pp. 39-44, 2005.
- [17] R. Fergus et al., —Removing Camera Shake from a Single Photograph, *ACM Transactions on Graphics*, vol. 25, no. 3, pp. 787-794, Jul, 2006.

- [18] O. Whyte et al., —Non-uniform Deblurring for Shaken Images,| International Journal of Computer Vision, vol. 98, no. 2, pp. 168-186, Jun, 2012.
- [19] P. Comon, and C. Jutten, Handbook of Blind Source Separation (Independent Component Analysis and Applications): Elsevier, 2010.
- [20] D. Vigliano et al., —Flexible Nonlinear Blind Signal Separation in the Complex Domain,| International Journal of Neural Systems, vol. 18, no. 2, pp. 105-122, Apr, 2008.
- [21] F. Cong et al., —Single-Trial Based Independent Component Analysis on Mismatch Negativity in Children,| International Journal of Neural Systems, vol. 20, no. 4, pp. 279-292, Aug, 2010.
- [22] L. S. Yuan, J. L. Quan, and H. Shum, —Image Deblurring With Blurred/Noisy Image Pairs,| ACM Transactions on Graphics, 2007.
- [23] Q. Shan, J. Jia, and A. Agarwala, —High-Quality Motion Deblurring From a Single Image,| ACM Transactions on Graphics, vol. 27, no. 3, pp. 10, Aug, 2008.
- [24] S. Cho, J. Wang, and S. Lee, —Handling Outliers in Non-Blind Image Deconvolution,| in International Conference on Computer Vision, New York, 2011, pp. 495-502.
- [25] O. Whyte, J. Sivic, and A. Zisserman, —Deblurring Shaken and Partially Saturated Images,| in International Conference on Computer Vision Workshops, New York, 2011.
- [26] M. Hirsch et al., —Fast Removal of Non-uniform Camera Shake,| in International Conference on Computer Vision, New York, 2011, pp. 463-470.
- [27] X. Yuquan et al., —Single-Image Blind Deblurring for Non-Uniform Camera Shake Blur,| in Proceedings of the 11th Asian conference on Computer Vision Daejeon, Korea, 2013, pp. 336-348.
- [28] A. Gupta et al., —Single Image Deblurring Using Motion Density Functions,| in 11th European Conference on Computer Vision, Heraklion, Crete, Greece, 2010, pp. 171-184.
- [29] M. S. C. Almeida, and L. B. Almeida, —Blind and Semi-Blind Deblurring of Natural Images,| IEEE Transactions on Image Processing, vol. 19, no. 1, pp. 36-52, Jan, 2010.
- [30] Y. P. Zhang, and T. Ueda, —Deblur of Radially Variant Blurred Image for Single Lens System,| IEEJ Transactions on Electrical and Electronic Engineering, vol. 6, pp. 7-16, 2011.
- [31] [70] D. Brunet, E. R. Vrscay, and Z. Wang, —On the Mathematical Properties of the Structural Similarity Index,| IEEE Transactions on Image Processing, vol. 21, no. 4, pp. 1488-1499, Apr, 2012.
- [32] Z. Wang, and Q. Li, —Information Content Weighting for Perceptual Image Quality Assessment,| IEEE Transactions on Image Processing, vol. 20, no. 5, pp. 1185-1198, May, 2011.
- [33] A. Khan, and H. Yin, —Efficient Blind Image Deconvolution Using Spectral Non-Gaussianity,| Integrated Computer-Aided Engineering, vol. 19, no. 4, pp. 331-340, 2012.
- [34] A. Khan, and H. J. Yin, "Spectral Non-gaussianity for Blind Image Deblurring," Intelligent Data Engineering and Automated Learning - Ideal 2011, Lecture Notes in Computer Science H. Yin, W. Wang and V. RaywardSmith, eds., pp. 144-151, Berlin: Springer-Verlag Berlin, 2011.
- [35] A. Mittal, A. K. Moorthy, and A. C. Bovik, —No-Reference Image Quality Assessment in the Spatial Domain,| IEEE Transactions on Image Processing, vol. 21, no. 12, pp. 4695-4708, Dec, 2012.
- [36] A. Mittal, A. K. Moorthy, and A. C. Bovik, "BRISQUE Software Release," 2011.
- [37] A. Mittal, R. Soundararajan, and A. C. Bovik, —Making a "Completely Blind" Image Quality Analyzer,| IEEE Signal Processing Letters, vol. 20, no. 3, pp. 209-212, Mar, 2013
- [38] A. Mittal, A. K. Moorthy, and A. C. Bovik. "NIQE Software Release," <http://live.ece.utexas.edu/research/quality/nique.zip>.
- [39] L. D. Thede et al., —A Comparison of Methods for the Optimization of VGA Colormaps,| Proceedings of Twenty-Fifth Southeastern Symposium on System Theory (SSST), pp. 508 - 512, 1993.
- [40] Y. Gao, A. Rehman, and Z. Wang, —CW-SSIM Based Image Classification,| in 18th IEEE International Conference on Image Processing, New York, 2011, pp. 1249-1252.
- [41] A. Rehman, and Z. Wang, —SSIM-Based Non-Local Means Image Denoising,| in 18th IEEE International Conference on Image Processing, New York, 2011, pp. 217-220.
- [42] Y. Bando, —Single-Shot Image Deblurring with Modified Camera Optics,| PhD dissertation, The Graduate School of Information Science and Technology The University of Tokyo 2009.
- [43] Y. Bando, —Single-Shot Image Deblurring with Modified Camera Optics I, The Graduate School of Information Science and Technology The University of Tokyo., 2009.
- [44] A. Agrawal, and Y. Xu, —Coded Exposure Deblurring: Optimized Codes for PSF Estimation and Invertibility,| in IEEE Conference on Computer Vision and Pattern Recognition, New York, 2009, pp. 2066-2073.